

# Analysis of a New Three-Dimensional Quadratic Chaotic System

Zeraoulia ELHADJ

Dept. of Mathematics, University of Tébessa, (12000), Algeria

zeraoulia @ mail.univ-tebessa.dz, zelhadj12 @ yahoo.fr

**Abstract.** *This paper has reported the finding of a new simple three dimensional quadratic chaotic system with three nonlinearities obtained by adding a cross-product nonlinear term to the first equation of the Lü system. Basic properties of the system have been analyzed by means of Lyapunov exponent spectrum and bifurcation diagram of an associated Poincaré map. This analysis shows that the system has complex dynamics with some interesting characteristics in which there are several periodic regions, but each of them has quite different periodic orbits. Shil'nikov's criterion is included and discussed.*

## Keywords

New chaotic attractors, three quadratic nonlinearities, modified Lü system; Lyapunov exponent spectrum, bifurcation diagram, Poincaré map.

## 1. Introduction

Several researchers have defined and studied quadratic 3-D chaotic systems. The first was Lorenz [1] in 1963, where he proposed a simple mathematical model of a weather system which was made up of three linked nonlinear differential equations, showing rates of change in temperature and wind speed. Some surprising results clearly showed the complex behavior from supposedly simple equations. Also, it has been noted that the behavior of this system of equations was sensitively dependent on the initial conditions of the model. He spelled out the implication of his discovery, saying it implied that if there were any errors in observing the initial state of the system which is inevitable in any real system, therefore, the prediction of a future state of the system was impossible. Later, Ruelle in 1979, when computer simulation came along, the first fractal shape identified took the form of a butterfly; it arose from graphing the changes in weather systems modeled by Lorenz. The Lorenz's attractor shows just how and why weather prognostication is so involved and notoriously wrong because of the butterfly effect. This amusing name reflects the possibility that a "butterfly in the Amazon might, in principal, ultimately alter the weather in Kansas".

Recently, chaos has been found to be very useful and has great potential in many technological disciplines such

as in information and computer sciences, power systems protection, biomedical systems analysis, flow dynamics and liquid mixing, encryption and communications, and so on [9], [7], [10]. As new applications of chaos theory the example is given in [10] where the adaptive synchronization with unknown parameters is discussed for a unified chaotic system by using the Lyapunov method and the adaptive control approach. Some communication schemes, including chaotic masking, chaotic modulation, and chaotic shift key strategies, are then proposed based on the modified adaptive method. In these schemes the transmitted signal is masked by chaotic signal or modulated into the system, which effectively blurs the constructed return map and can resist this return map attack. The driving system with unknown parameters and functions is almost completely unknown to the attackers, so it is more secure to apply this method into the communication.

In this paper a new continuous-time three-dimensional autonomous system is presented as follows:

$$\begin{cases} \dot{x} = a(y-x) + yz, \\ \dot{y} = cy - xz, \\ \dot{z} = xy - bz, \end{cases} \quad (1)$$

where we add a cross-product nonlinear term  $yz$  to the first equation of the Lü system [4], where the parameters  $a, b, c$  are assumed to be positive along this study. Note that the adding of a cross-product nonlinear term is not a universal method for chaotifying a 3-D quadratic system. Moreover, presented system (1) has three nonlinear terms and thus definitely does not belong to the algebraically simple chaotic flows, but there are 3-D systems more complicated than system (1), and they are suitable for practical realization as an electronic circuit [13]. The evolution of the new system (1) is analyzed by means of Lyapunov exponent spectrum and bifurcation diagram for an associated Poincaré map. This analysis shows that the system has complex dynamics with some interesting characteristics in which there are several periodic regions, but each of them has quite different periodic orbits. Note that the system (1) is symmetric under the coordinate transform  $(x, y, z) \rightarrow (-x, -y, z)$ , this transformation persists for all values of the system parameters. Therefore for system (1), the divergence of the flow is given by  $\nabla V = \partial x' / \partial x + \partial y' / \partial y + \partial z' / \partial z = -(a - c + b)$

then the system (1) is dissipative when  $a - c + b > 0$ , and it converges to a set of measure zero exponentially. The fixed points of system (1) has the form  $\left(x = \frac{-aby}{-ab + y^2}, y, z = \frac{-ay^2}{ab - y^2}\right)$ , if  $y^2 \neq ab$ , where  $y$  is the real solution of the equation

$$y \left( cy^4 - (2abc + a^2b)y^2 + a^2b^2c \right) = 0. \quad (2)$$

Obviously,  $P_0 = (0,0,0)$  is an equilibrium point, and the other non zero equilibria are given by  $P_i = (x_i, y_i, z_i)$ ,  $i = 1, 2, 3, 4$  where

$$\begin{aligned} y_1 &= \sqrt{\frac{2abc + a^2b + \sqrt{b^2a^3(a+4c)}}{2c}}, \\ y_2 &= -\sqrt{\frac{2abc + a^2b + \sqrt{b^2a^3(a+4c)}}{2c}}, \\ y_3 &= \sqrt{\frac{2abc + a^2b - \sqrt{b^2a^3(a+4c)}}{2c}}, \text{ and} \\ y_4 &= -\sqrt{\frac{2abc + a^2b - \sqrt{b^2a^3(a+4c)}}{2c}}. \end{aligned}$$

For these equilibria, their stabilities can be estimated via numerical computation, which is not further discussed here. On the other hand, it is easy to verify that system (1) and all other existing three-dimensional quadratic systems, for example Lorenz system [1], Chen system [3], Lü system [4], Lorenz system family [5]... are not topologically equivalent since the former has five equilibria but the other systems have only three. For the system given in [6], it is straightforward (but somewhat tedious) to verify that there is no non-singular (linear or nonlinear) coordinate transform (i.e. diffeomorphism) that can convert such system to other.

## 2. The Type of Chaos in the Model

Homoclinic and heteroclinic orbits arise in the study of bifurcation and chaos phenomena, as well as their applications as in mechanics, biomathematics and chemistry [14], [15]. In some cases it is necessary to determine the nature or the type of chaotic behaviors resulting from a dynamical system, one of the commonly agreeable analytic criteria for proving chaos in autonomous systems is the work of Shiřnikov [16], [17], the resulting chaos is called horseshoe type or *Shiřnikov chaos*.

Consider the third-order autonomous system  $x' = f(x)$  where the vector field  $f: \mathfrak{R}^3 \rightarrow \mathfrak{R}^3$  belongs to class  $C^r (r \geq 1)$ , and  $x \in \mathfrak{R}^3$  is the state variable of the system, and  $t \in \mathfrak{R}$  is the time. Suppose that  $f$  has at least an equilibrium point  $P$ . The point  $P$  is called a hyperbolic saddle focus for system (1), if the eigenvalues of the Jacobian  $A = Df(P)$  are  $\gamma, \alpha + i\beta$  where  $\alpha\gamma < 0, \beta \neq 0$ . A homoclinic orbit  $\gamma(t)$  refers to a bounded trajectory of system (1) that is doubly asymptotic to an equilibrium point  $P$  of the system, i.e.  $\lim_{t \rightarrow +\infty} \gamma(t) = P = \lim_{t \rightarrow -\infty} \gamma(t) = P$ . A heteroclinic orbit  $\delta(t)$ , is similarly de-

finied except that there are two distinct saddle foci  $P_1$ , and  $P_2$ , being connected by the orbit, one corresponding to the forward asymptotic time, and the other, to the reverse asymptotic time limit, i.e.  $\lim_{t \rightarrow +\infty} \delta(t) = P_1$ , and  $\lim_{t \rightarrow -\infty} \delta(t) = P_2$ .

The heteroclinic Shiřnikov method, namely, the Shiřnikov criterion for the existence of chaos, is summarized in the following theorem:

**Theorem.1.** Suppose that two distinct equilibrium points; denoted by  $P_1$ , and  $P_2$  respectively, of the system  $x' = f(x)$  are saddle foci, whose characteristic values  $\gamma_k, \alpha_k + i\beta$  ( $k = 1, 2$ ) satisfy the following Shiřnikov inequalities  $\alpha_1\alpha_2 > 0$ , or  $\gamma_1\gamma_2 > 0$ . Suppose also that there exists a heteroclinic orbit joining  $P_1$ , and  $P_2$ , then, the system  $x' = f(x)$  has both Smale horseshoes and the horseshoe type of chaos.

For the values  $a = 36, b = 3, c = 25$ , system (1) has the chaotic attractor shown in Fig. 3 (b). In this case, the equilibria and their eigenvalues are given by:

$$\begin{cases} P_0 = (0, 0, 0), \{-36, -3, 25\}, \\ P_1 = (-8.6603, 18.355, -52.986), \{-36, 726, 11.363 \pm 21.831i\}, \\ P_2 = (8.6603, -18.355, -52.986), \{-36, 726, 11.363 \pm 21.831i\}, \\ P_3 = (8.6603, 5.884, 16.986), \{-23.648, 4.824 \pm 16.682i\}, \\ P_4 = (-8.6603, -5.884, 16.986), \{-23.648, 4.824 \pm 16.682i\}. \end{cases} \quad (3)$$

Thus, one can easily obtain that all  $(P_i)_{1 \leq i \leq 4}$  are of hyperbolic saddle focus type, but the point  $P_0$  is not of this type because its eigenvalues are  $-36, -3, 25$ , then, there is no homoclinic or heteroclinic orbits of Shiřnikov type that is doubly asymptotic to the equilibrium  $P_0$ . Hence, for the points  $(P_i)_{1 \leq i \leq 4}$ , there is a possibility to get a homoclinic or heteroclinic orbit for the system (1). Fig. 1 shows a numerical approximation of the heteroclinic orbit joining  $P_3$  and  $P_4$  with the parameter values  $a = 36, b = 3, c = 25$ . The orbit is obtained using the so-called trial-and-error method given in [11], in which we start many initial conditions in a small neighborhood of an equilibrium point and follow the trajectories for a fixed but small time to see if they return to the vicinity of the equilibrium. Note that in this numerical method, the data are calculated in double precision.

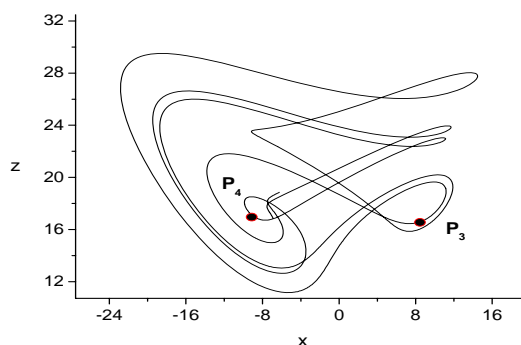


**Fig. 1.** Numerical approximation of the heteroclinic orbit joining  $P_3$  and  $P_4$  in the system (1) with the parameter values  $a = 36, b = 3, c = 25$ .

As a final result in this section, the chaotic attractor presented by system (1) has both Smale horseshoes and the horseshoe type of chaos.

### 3. Numerical Analysis

In this section, the dynamical behaviors of the system (1) are investigated numerically where we use an appropriate Poincaré section where the resulting points  $\{y_n\}_{n \in \mathbb{N}}$  are computed using the Hénon method [12], and a set of one of them is recorded after transients have decayed and plotted versus the desired parameter. The calculations of limit sets of the system (1) were performed using a fourth Runge-Kutta algorithm [12] with a constant step size  $\Delta t = 10^{-3}$ , then, to determine the long-time behavior and chaotic regions, we numerically computed the largest Lyapunov exponent [12]. Note that in all these numerical methods, the data are calculated in double precision. When we fix  $b = 3$ ,  $c = 25$ , and vary  $a \geq 0$ , Fig. 2 (b) shows the spectrum of the largest Lyapunov exponent of system (1) with respect to the parameter  $a \geq 0$ : Obviously, when  $a \in [32.2, 46.7]$ , the maximum Lyapunov exponent is positive, thus, the new system (1) has chaotic attractors. Figs. 3, 4, show different phase portraits of system (1) where  $a = 30$ , and  $a = 36$ , and  $a = 46$ , and  $a = 50$ , respectively.

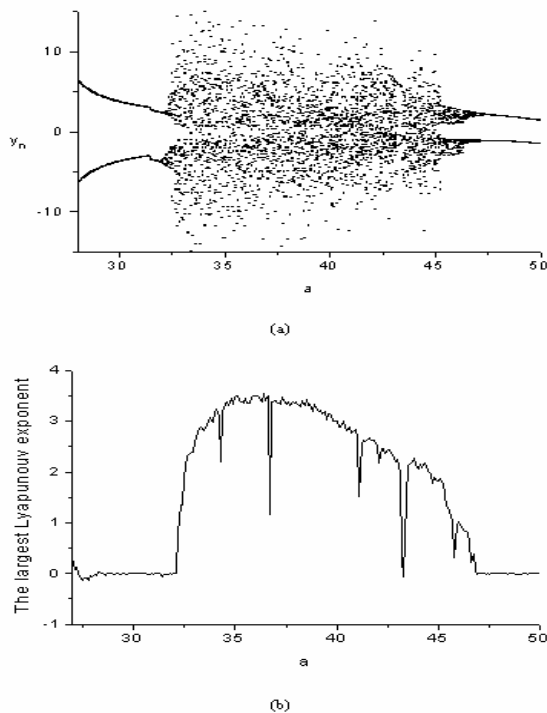


**Fig. 2.** (a) Bifurcation diagram of the variable  $y_n$  plotted versus control parameter  $a \in [28, 50]$ , with  $b=3$ ,  $c=25$ . (b) Variation of the largest Lyapunov exponent of system (1) versus the parameter  $a \in [28, 50]$ , with  $b=3$ ,  $c=25$ .

For drawing the bifurcation diagram we used an appropriate Poincaré section  $\Sigma$  defined by:

$$\Sigma = \{(y, z) \in \mathbb{R}^2 / x=0, \} \tag{4}$$

The result is shown in Fig.2 (a).

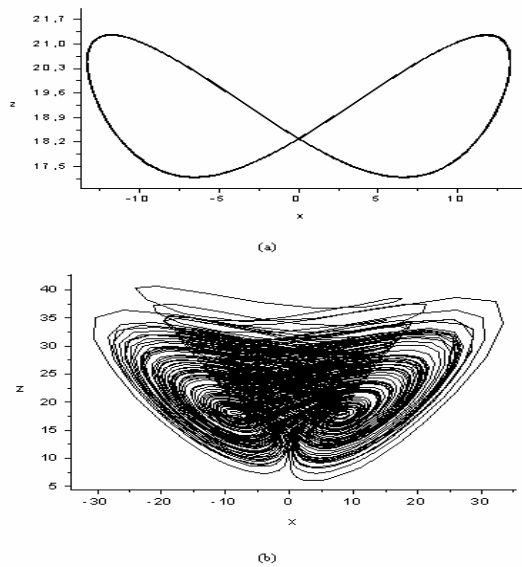


**Fig. 3.** Projection into the  $x-z$  plane of some phases portrait obtained from system (1) for:  $b=3$ ,  $c=25$ , and (a)  $a=30$ , (b)  $a=36$ .

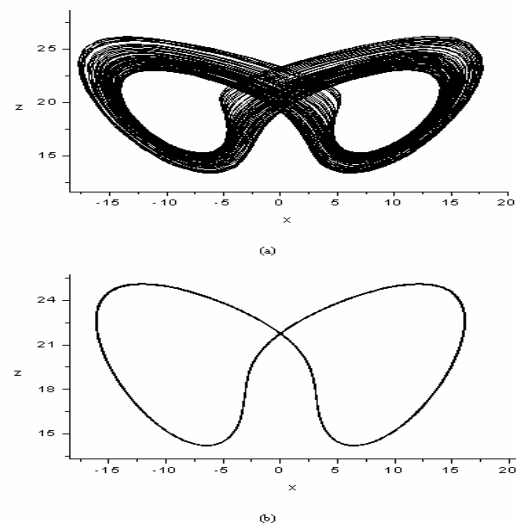


**Fig. 4.** Projection into the  $x-z$  plane of some phases portrait obtained from system (1) for:  $b=3$ ,  $c=25$ , and (a)  $a=46$ , (b)  $a=50$ .

With  $a$  increasing, Fig. 2 (a) clearly shows the creation of chaos from period-doubling bifurcations. In the other hand, there is a degeneration process of the new chaotic attractor to the periodic solution region, where the system orbit degenerates through reverse period-doubling bifurcations. In fact, the whole evolution process contains two distinct processes: First, the new chaotic attractor is gradually degenerating to periodic solution regions. Second, the degeneration process is often suddenly changed by turning and location of the system orbit. When we fix  $a = 36$ ,  $c = 25$ , and vary  $b \geq 0$ , Fig.5 (b) shows that when  $b \in [0.4, 6.1]$ , system (1) is chaotic with a positive Lyapunov exponent (for example, with  $b = 2$ ;  $b = 5.6$ , and  $b = 11$ , the phase portraits are shown in Figs.6(a), 6(b)), and 6(c) respectively.

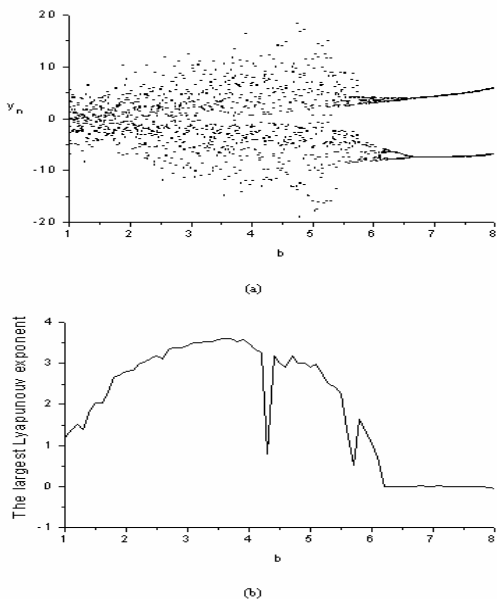


**Fig. 5.** (a) Bifurcation diagram of the variable  $y_n$  plotted versus  $b \in [1, 8]$ , with  $a = 36, c = 25$ .  
 (b) Variation of the largest Lyapunov exponent of system (1) versus the parameter  $b \in [1, 8]$  with  $a = 36, c = 25$ .

For drawing the bifurcation diagram with respect to  $b$  we use again the same Poincaré section  $\Sigma$  defined by equation (4); the result is shown in Fig. 5 (a).

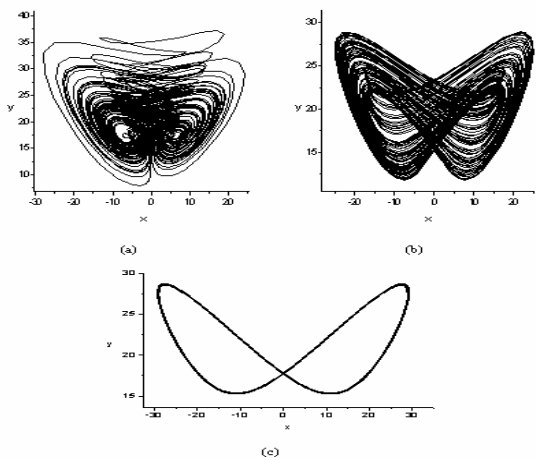


**Fig. 6.** Projection into the  $x-z$  plane of the new chaotic attractors obtained from system (1) for:  $a = 36, c = 25$ , and (a)  $b = 2$ , (b)  $b = 5.6$ , (c)  $b = 11$ .

With  $b$  increasing, Fig.5 (a), clearly shows the degeneration process of the new chaotic attractor to the periodic solution region as shown for example in Fig. 6(c), where the system orbit degenerates through reverse period-doubling bifurcations. In summary the dynamics of the system (1) with respect to  $b$  is similar to the previous one with respect to  $a$ , especially the whole evolution process contains the two distinct processes mentioned above.

When we fix  $a = 36, b = 3$ , and vary  $c \geq 0$ , Fig. 7 (b) shows the variation of the largest Lyapunov exponent of the system (1) versus the parameter  $c \in [15, 33]$ : When

$c \in [9.8, 10.7]$ , and when  $c \in [16.9, 28.4]$ , the system is chaotic with a positive Lyapunov exponent, for example, with  $c = 9.8, c = 10.8, c = 11.5, c = 17, c = 19$ , and  $c = 29$ , the phase portraits are shown in Figs. 8(a), 8(b), 9(a), 9(b), 10(a), 10(b) respectively.

For drawing the bifurcation diagram we used the same Poincaré section  $\Sigma$  defined by equation (4).

With  $c$  increasing in the interval  $[16.9, 28.4]$ , Fig. 7(a) clearly shows also the same processes of the creation of chaos from period-doubling bifurcations and the degeneration process of the new chaotic attractor to the periodic solution regions via reverse period doubling bifurcation as shown in Figs. 8, 9 and 10. In summary the dynamics of the system (1) with respect to  $c$  is similar to the previous one with respect to  $a$  and  $b$ , especially the whole evolution process contains the two distinct processes mentioned above.

From Figs. 3(a), 4(b), 6(c), 8(b), 9(a), and 10(b), we remark that periodic regions do not share the same dynamic characteristics, in which there are several periodic regions, but each of them has quite different periodic orbits. On the other hand, the dynamics of the system (1) is different from that of the Lü system [4] since system (1) contains more nonlinear terms and equilibria, and brings to different locations of nonzero equilibria and different dynamical properties, even taking the same parameters. The same task is with the other systems mentioned above, especially, the one given in [6].

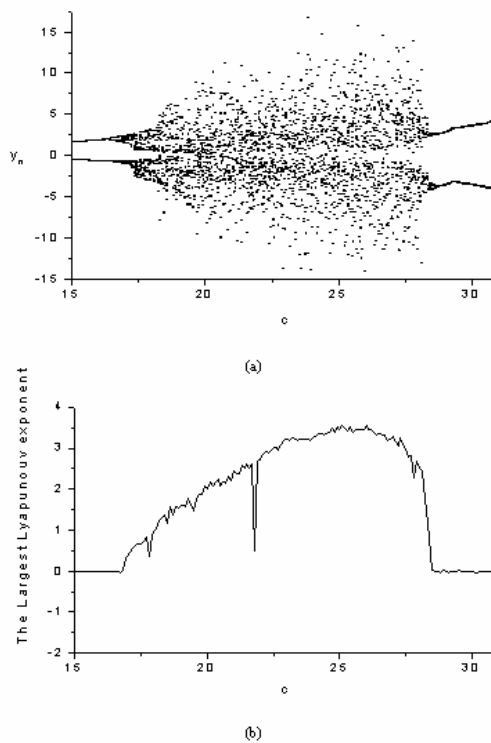


**Fig. 7.** (a) Bifurcation diagram of the variable  $y_n$  plotted versus the parameter  $c \in [15, 31]$ , with  $a = 36$ , and  $b = 3$ .  
 (b) Variation of the largest Lyapunov exponent of system (1) versus  $c \in [15, 31]$ , with  $a = 36$ , and  $b = 3$ .

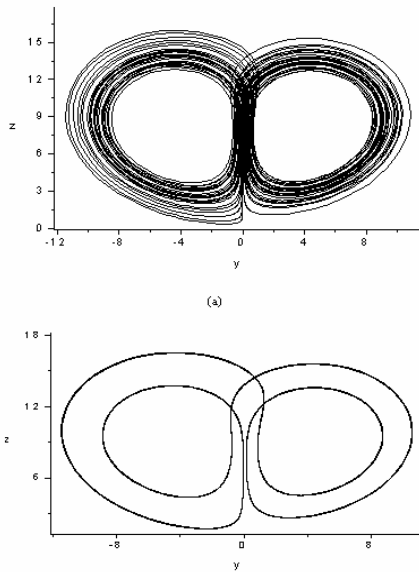


**Fig. 8.** Projection into the  $y$ - $z$  plane of some phases portrait obtained from system (1) for:  $a=36$ ,  $b=3$ , and (a)  $c=9.8$ , (b)  $c=10.8$ .

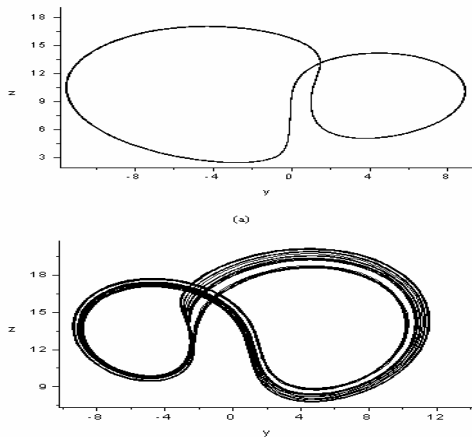


**Fig. 9.** Projection into the  $y$ - $z$  plane of some phases portrait obtained from system (1) for:  $a=36$ ,  $b=3$ , and (a)  $c=11.5$ , (b)  $c=17$ .

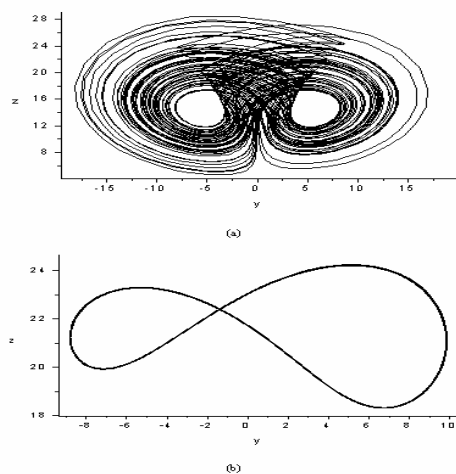


**Fig. 10.** Projection into the  $y$ - $z$  plane of some phases portrait obtained from system (1) for:  $a=36$ ,  $b=3$ , and (a)  $c=19$ , (b)  $c=29$ .

## 4. Conclusion

We have reported some results about a new three-dimensional quadratic chaotic system with three nonlinearities obtained by adding a cross-product nonlinear term to the first equation of the Lü system. Basic properties of the system have been analyzed by means of Lyapunov exponent spectrum and bifurcation diagram of an associated Poincaré map. Shilnikov's criterion is also included and discussed.

## References

- [1] LORENZ, E. N. Deterministic nonperiodic flow. *J. Atmos. Sc.*, 1963, vol. 20, p. 130 - 141.
- [2] RÖSSLOR, O. E. An equation for continuous chaos. *Phys. Lett. A*, 1976, vol. 57, p. 397 - 398.
- [3] CHEN, G., UETA, T. Yet another chaotic attractor. *Int. J. Bifur. Chaos*, 1999, vol. 9, p. 1465 - 1466.
- [4] LÜ, J. H., CHEN, G. A new chaotic attractor coined. *Int. J. Bifurcat. Chaos*, 2002, vol. 12, p. 659 - 661.
- [5] LÜ, J. H., CHEN, G., CHENG, D., CELIKOVSKY, S. Bridge the gap between the Lorenz system and the Chen system. *Int. J. Bifur. Chaos*, 2002, vol. 12, no. 12, p. 2917 - 2926.
- [6] QI, G., CHEN, G., DU, S. Analysis of a new chaotic system. *Physica A*, 2005, vol. 352, p. 295 - 308.
- [7] CHEN, G. *Controlling Chaos and Bifurcations in Engineering System*. CRC Press, Boca Raton, FL, 1999.
- [8] ELHADJ, Z., EDDINE, H. N. A generalized model of some Lorenz-type and quasi-attractors type strange attractors in three-dimensional dynamical systems. *International Journal of Pure & Applied Mathematical Sciences*, 2005, vol. 2, no. 1, p. 67 - 76.
- [9] CHEN, G., DONG, X. *From Chaos to Order: Methodologies, Perspectives and Applications*. (World Scientific, Singapore), 1998.
- [10] YU, W. W., CAO, J., WONG, K. W., LÜ, J. New communication schemes based on adaptive synchronization. *Chaos*, 2007, vol. 17, no. 3, p. 033 - 114.
- [11] SPROTT, J. C. *Chaos and Time-Series Analysis*. Oxford University Press, Oxford, 2003.
- [12] PARKER, T.S., CHUA, L.O. *Practical Numerical Algorithms for Chaotic Systems*. Springer Verlag, New York, 1989.
- [13] YU, S. M., LÜ, J., CHEN, G. Theoretical design and circuit implementation of multi-directional multi-torus chaotic attractors. *IEEE Trans. on Circuits and Systems I*, 2007, vol. 54, no.9, p. 2087 - 2098.
- [14] AULBACH, B., FLOCKERZI, D. The past in short hypercycles. *J. Math. Biol.*, 1989, vol. 27, p. 223 - 231.
- [15] BALMFORTH, N. J. Solitary waves and homoclinic orbits. *Annual review of fluid mechanics*, 1995, vol. 27, p. 335 - 373, Annual Reviews, Palo Alto, CA.
- [16] SHILNIKOV, L. P. A case of the existence of a countable number of periodic motions. *Sov. Math. Doklady*, 1965, vol. 6, p. 163 - 166 (translated by S. Puckette).
- [17] SHILNIKOV, L. P. A contribution of the problem of the structure of an extended neighborhood of rough equilibrium state of saddle-focus type. *Math. U.S.S.R.Sbornik*, 1970, vol. 10, p. 91-102 (translated by F. A. Cezus).